

Synthesis and UV–Vis, Electrochemical, Spectroelectrochemical, and Intervalence Characterization of Bis(bipyridyl)osmium(II) Complexes Bound to Dipyrido[2,3-*a*:2',3'-*h*]phenazine (dpop)

Ronald R. Ruminski,* Donna Serveiss, and Martin Jacques

Department of Chemistry, University of Colorado at Colorado Springs, Colorado Springs, Colorado 80933-7150

Received November 1, 1994

Introduction

Osmium(II) and ruthenium complexes with polypyridyl ligands display intense metal to ligand charge transfer (MLCT) transitions in the visible spectrum. This property in conjunction with favorable photostability and electrochemical characteristics make the systematic preparation and study of these complexes important for photo initiated energy transfer or sensitization processes.¹ Some research initiatives control photophysical and redox properties of complexes by substituent variation on the polypyridine ligands or sequential addition of various ligands on the metallic center.² Our research efforts attempt to control these properties through the preparation of complexes with bridging ligands (BL) that allow greater mixing of the metal- $(d\pi)$ and $BL(\pi^*)$ orbitals.³ We wish to report the synthesis and characterization of the first Os(II) complexes with dipyrido[2,3-*a*:2',3'-*h*]phenazine (dpop). The $[(bpy)_2Os(dpop)](PF_6)_2$ and $[(bpy)_2Os(dpop)](PF_6)_4$ complexes have lower energy MLCT absorptions and larger Os(II)–BL–Os(II) electrochemical interactions than have been recently reported using similar BL.^{4–10}

Experimental Section

Instrumentation. Visible–ultraviolet electronic absorption spectra were recorded on a Varian DMS 300 Spectrophotometer, and near-infrared electronic absorption spectra were recorded on a Beckman 5240 spectrophotometer, with matching quartz cells. D₂O (99.8% D) was obtained from Aldrich Chemicals. Cyclic voltammograms were recorded in CH₃CN with 0.10 M tetrabutylammonium hexafluorophosphate as the supporting electrolyte using a Bio Analytical Systems CV-1B cyclic voltammograph system as previously described.³ Potentials are reported vs Ag/AgCl(–0.045 V vs SCE). Spectroelectrochemi-

cal experiments were conducted at Virginia Polytechnic Institute and State University on equipment previously described.¹¹

Materials. Reagent grade compounds were used for preparations described in this work. Elemental analyses were performed by Atlantic Microlab, Atlanta, GA.

Synthesis. The dpop ligand was prepared according to the literature¹² with minor modifications as previously described.¹³ The $[(bpy)_2Os(Cl)_2]$ reactant was also prepared according to the literature.⁶

$[(bpy)_2Os(dpop)](PF_6)_2 \cdot H_2O$. A 0.101 g (0.177 mmol) sample of $[(bpy)_2Os(Cl)_2]$ and 0.0800 g (0.284 mmol) dpop were mixed in 30–40 mL of ethylene glycol and heated at reflux under argon for 8 h. After cooling to room temperature, an equal volume of saturated aqueous KPF₆ was added to induce precipitation. The solid was collected on a fine porosity filter funnel and was air-dried overnight. The precipitate was then washed with chloroform to remove excess unreacted dpop and again air-dried. The solid was then dissolved in a minimum volume of acetone (approximately 100 mL), and the red solution was suction filtered through the funnel. The solution was chromatographed on a 15 cm (length) Al₂O₃ column using acetone. Initial volumes of eluant were slightly yellow and contained uncomplexed dpop. The red product that eluted next was collected, was rotary evaporated to a minimum volume, and was precipitated by addition of NH₄PF₆(s) and then diethyl ether. The chromatographic process was repeated two additional times using a shorter (4 cm) alumina column. After final collection, the product was washed with a minimum volume of water to remove excess NH₄PF₆, and vacuum dried at 40 °C. Yield: 0.44 g (4.03×10^{-5} mol), 23% based on $[(bpy)_2Os(Cl)_2]$ as limiting reactant. Anal. Calcd for $[(bpy)_2Os(dpop)](PF_6)_2 \cdot H_2O$, mol mass 1092.80 amu: C, 41.76; H, 2.55; N, 10.25. Found: C, 41.70; H, 2.59; N, 10.12.

$[(bpy)_2Os(dpop)](PF_6)_4$. A 0.100 g (0.174 mmol) sample of $[(bpy)_2Os(Cl)_2]$ and 0.0210 g (0.0744 mmol) dpop were mixed in 30–40 mL of ethylene glycol and heated at reflux under argon for 24 h. After cooling to room temperature, an equal volume of saturated aqueous KPF₆ was added to induce precipitation. The solid was collected on a fine porosity filter funnel and was dried overnight. The solid was then dissolved in a minimum volume of acetone and the green solution suction filtered through the funnel. The solution was chromatographed on a 15 cm (length) Al₂O₃ column using 0.5 g of NH₄PF₆/200 mL of acetone. An olive green band was collected and rotary evaporated to a minimum volume, and the product was precipitated by addition of diethyl ether. The chromatographic process was repeated a second time. After final collection, the product was washed with a minimum volume of water to remove NH₄PF₆, and vacuum dried at 40 °C. Yield: 0.0890 g (4.77×10^{-5} mol), 55% based on dpop as the limiting reactant. Anal. Calcd for $[(bpy)_2Os(dpop)](PF_6)_4$, mol mass 1867.28 amu: C, 37.30; H, 2.27; N, 9.00. Found: C, 37.29; H, 2.30; N, 8.93.

Results and Discussion

Electrochemistry. Electrochemical data for the mono and bimetallic $[(bpy)_2Os]_{1,2}(dpop)^{2+,4+}$ complexes in acetonitrile obtained by cyclic voltammetry is summarized in Table 1. The monometallic $[(bpy)_2Os(dpop)]^{2+}$ ion displays one reversible oxidation and four reversible reduction waves between +1.5

- (1) (a) Scandola, F.; Bignozzi, C. A. *Photosensitization and Photocatalysis Using Inorganic and Organometallic Compounds*; Kluwer Academic Publishers: Dordrecht, The Netherlands, 1993; pp 161–216. (b) Balzani, V., Ed. *Supramolecular Photochemistry*; NATO ASI Series C214; Reidel: Dordrecht, The Netherlands 1987. (c) Fox, M. A.; Chanon, M., Eds. *Photoinduced Electron Transfer*; Elsevier, New York, 1988. (d) Juris, A.; Barigelletti, S.; Campagna, S.; Balzani, V.; Belser, P.; von Zelewski, A. *Coord. Chem. Rev.* **1988**, *84*, 85.
- (2) Anderson, P. A.; Strouse, G. F.; Treadway, J. A.; Keene, F. R.; Meyer, T. J. *Inorg. Chem.* **1994**, *33*, 3863.
- (3) Johnson, J. E. B.; Ruminski, R. R. *Inorg. Chim. Acta* **1993**, *208*, 231.
- (4) Juris, A.; Balzani, V.; Campagna, S.; Denti, G.; Serroni, S.; Frei, G.; Gudel, H. *Inorg. Chem.* **1994**, *33*, 1491.
- (5) Reference deleted in proof.
- (6) Richter, M. M.; Brewer, K. J. *Inorg. Chim. Acta* **1991**, *180*, 125.
- (7) Richter, M. M.; Brewer, K. J. *Inorg. Chem.* **1993**, *32*, 2827.
- (8) Denti, G.; Serroni, S.; Sabitino, L.; Ciano, M.; Recevuto, V.; Campagna, S. *Gazz. Chim. Ital.* **1991**, *121*, 37.
- (9) Haga, M.; Matsumura-Inoue, T.; Yamabe, S. *Inorg. Chem.* **1987**, *26*, 4148.
- (10) Kalyanasundaram, K.; Nazeeruddin, Md. K. *Inorg. Chim. Acta* **1990**, *171*, 213.

- (11) Brewer, K. J.; Lumpkin, R. S.; Otovos, J. W.; Spreer, L. O.; Calvin, M. *Inorg. Chem.* **1989**, *28*, 4446.
- (12) Pfeiffer, P. R.; Case, F. H. *J. Org. Chem.* **1966**, *31*, 3384.
- (13) Ruminski, R. R.; DeGross, C.; Smith, S. J. *Inorg. Chem.* **1991**, *31*, 3325.

Table 1. Electrochemical Data for Some Osmium(II) Bipyridyl Ions^a

monometallic complexes	$E_{1/2}(2)$	$E_{1/2}(1)$	$\Delta E(2-1)$	$E_{1/2}^{0/1-}$	$E_{1/2}^{1-/-2-}$	$E_{1/2}^{2-/-3-}$	$E_{1/2}^{3-/-4-}$	ref
$(\text{bpy})_2\text{Os}(\text{dpop})^{2+}$		1.04		-0.59	-1.23	-1.40	-1.68	this work
$(\text{bpy})_2\text{Os}(2,3\text{-dpp})^{2+}$		0.94		-1.02	-1.38	-1.58		6
$(\text{bpy})_2\text{Os}(\text{dpq})^{2+}$		0.99		-0.76	-1.26	-1.57		6
$(\text{bpy})_2\text{Os}(\text{dpb})^{2+}$		1.00		-0.61	-1.16	-1.55		6
bimetallic complexes	$E_{1/2}(2)$	$E_{1/2}(1)$	$\Delta E(2-1)$	$E_{1/2}^{0/1-}$	$E_{1/2}^{1-/-2-}$	$E_{1/2}^{2-/-4-}$	$E_{1/2}^{4-/-6-}$	ref
$((\text{bpy})_2\text{Os})_2(\text{dpop})^{4+}$	1.40	1.04	0.36	-0.21	-0.81	-1.38(2)	-1.7(2)	this work
$((\text{bpy})_2\text{Os})_2(2,3\text{-dpp})^{4+}$	1.22	0.91	0.31	-0.68	-1.06			7, 8
$((\text{bpy})_2\text{Os})_2(\text{dpq})^{4+}$	1.28	0.98	0.30	-0.44	-1.03			7, 8
$((\text{bpy})_2\text{Os})_2(\text{dpb})^{4+}$	1.30	0.98	0.32	-0.33	-0.85			7, 8

^a Recorded in $\text{CH}_3\text{CN}/0.10\text{M Bu}_4\text{NPF}_6$ vs Ag/AgCl for comparison with previously reported values.

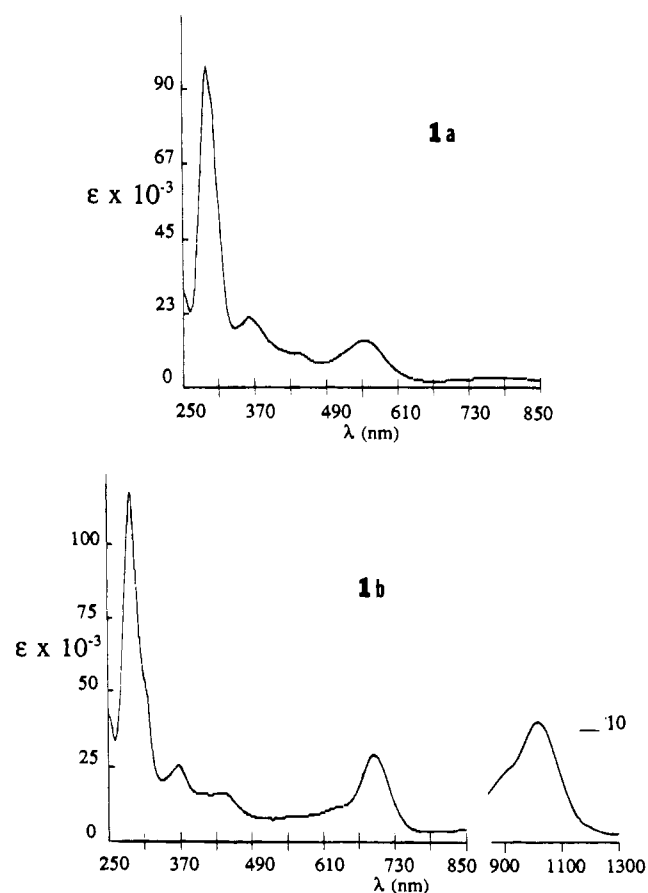
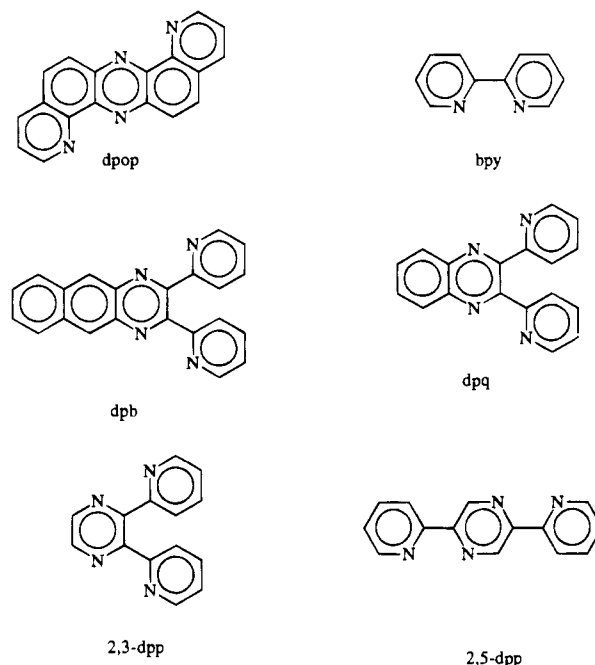


Figure 1. Electronic absorption spectra of (a) $[(\text{bpy})_2\text{Os}(\text{dpop})]^{2+}$ and (b) $[((\text{bpy})_2\text{Os})_2(\text{dpop})]^{4+}$ ions in acetonitrile.

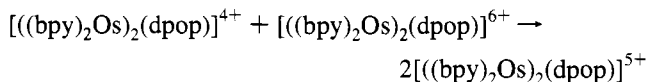
and -1.8 V. The $\text{Os}^{2+/3+}$ couple at $E_{1/2} = +1.04$ V vs Ag/AgCl is at the positive end of the range of values previously reported for $[(\text{bpy})_2\text{Os}(\text{BL})]^{2+/3+}$ complexes with similar BL (BL = 2,3-bis(2-pyridyl)pyrazine (2,3-dpp), 2,3-bis(2-pyridyl)quinoxaline (dpq), and 2,3-bis(2-pyridyl)benzoquinoxaline (dpb) (Chart 1)).⁶ The value of the potential supports the observation that the change in ligand field about the Os center caused by slight modification of the BL produces only small shifts in the $\text{Os}^{2+/3+}$ potential.⁶ Comparative reduction potentials for uncomplexed bridging ligands including dpop and for bpy show the bridging ligand is more electronegative than bpy. The least negative reduction waves at -0.59 and -1.23 V are therefore assigned as $\text{dpop}^{0/-}$ reductions. The third and fourth reductions of $[(\text{bpy})_2\text{Os}(\text{dpop})]^{2+}$ at -1.40 and -1.68 V are attributed to individual $\text{bpy}^{0/-}$ reductions, in agreement with previous assignments for $\text{bpy}^{0/-}$ processes.⁶

The bimetallic $[((\text{bpy})_2\text{Os})_2(\text{dpop})]^{4+}$ complex ion displays two reversible oxidation waves and multiple reduction waves (Table 1). The two reversible $\text{Os}^{2+/3+}$ processes are at slightly

Chart 1

more positive potential than those reported for other bimetallic osmium complexes.^{6,7} It has been shown that the electrochemical separation of the two separate one electron $\text{Os}^{2+/3+}$ oxidations defined as $\Delta E_{1/2}(2-1)$ is related to the structural and electronic properties of the bridging ligand.¹⁴⁻¹⁷ The $\Delta E_{1/2}(2-1)$ value of 360 mV is 40–60 mV larger than values for similar bimetallic $[((\text{bpy})_2\text{Os})_2(\text{BL})]^{4+}$ (BL = 2,3-dpp, dpq, and dpb) complexes.

The comproportionation constant K_{com} , for the reaction



is calculated from the formula $e^{(\Delta E_{1/2}(2-1)/25.69)}$ ($\Delta E_{1/2}(2-1) = 360$ mV, $T = 298$ K), as 1.2×10^6 . This is larger than K_{com} values reported for $[((\text{bpy})_2\text{Os})_2(\text{BL})]^{4+}$ (BL = 2,3-dpp, dpq, and dpb) that range between 2.6×10^5 and 1.2×10^5 ,⁷ but still within the region of class II systems as described by Robin and Day.¹⁸ The larger $\Delta E_{1/2}(2-1)$ and K_{com} values indicate greater mixing of the $\text{dpop}(\pi^*)$ and $\text{Os}(d\pi)$ orbitals resulting in a more

(14) Fuchs, Y.; Lofters, S.; Dieter, T.; Shi, W.; Morgan, R.; Streckas, T.; Gafney, H.; Baker, D. *J. Am. Chem. Soc.* **1987**, *109*, 2691.

(15) Goldsby, K. A.; Meyer, T. J. *Inorg. Chem.* **1984**, *23*, 3002.

(16) Creutz, C. *Prog. Inorg. Chem.* **1983**, *30*, 1.

(17) Barigelletti, F.; Juris, A.; Balzani, V.; Belser, P.; von Zelewsky, A. *J. Phys. Chem.* **1987**, *91*, 1095.

(18) Robin, M. B.; Day, P. *Adv. Inorg. Radiochem.* **1967**, *10*, 247.

strongly coupled Os centers in the bimetallic $[(\text{bpy})_2\text{Os}]_2(\text{dpop})^{4+}$ complex ion.

Two reversible reduction waves at -0.21 and -0.81 V vs Ag/AgCl for the $[(\text{bpy})_2\text{Os}]_2(\text{dpop})^{4+}$ complex are attributed to $\text{dpop}^{0/-2-}$ reductions. Although it is difficult to definitively determine one- or two-electron processes, based on cyclic voltammogram wave heights, broad wave forms, and $E_{1/2} = E_p^{\text{an}} - E_p^{\text{cat}}$ values of 100 mV, an additional reduction at -1.38 V may be attributed to two $\text{bpy}^{0/-}$ reductions on individual Os centers. A similar broad wave was observed for the $[(\text{bpy})_2\text{Os}]_2(\text{dpb})^{4+}$ complex ion upon the third and fourth reductions. An additional reduction wave near -1.7 V is obscured due to adsorption and is most likely due to the second set of individual $\text{bpy}^{0/-}$ reductions on remote Os centers. The coordination of the second $(\text{bpy})_2\text{Os}^{2+}$ fragment on the $[(\text{bpy})_2\text{Os}(\text{dpop})]^{2+}$ complex causes a positive shift of 380 mV for the $\text{dpop}^{0/-}$ reduction. This result is primarily due to the stabilization of the $\text{dpop}(\pi^*)$ orbitals on the bimetallic complexes compared to the $\text{dpop}(\pi^*)$ orbitals on monometallic complex.

Electronic Absorption Spectroscopy. The UV-visible electronic absorption spectra of the $[(\text{bpy})_2\text{Os}(\text{dpop})]^{2+}$ and $[(\text{bpy})_2\text{Os}]_2(\text{dpop})^{4+}$ ions in CH_3CN are summarized in Table 2 and shown in Figure 1. In general, the complexes exhibit $\text{Os}(\text{d}\pi) \rightarrow \text{dpop}(\pi^*)$ MLCT absorptions that are red shifted in comparison to mono and bimetallic Os(II) complexes bound to 2,3-dpp, 2,5-dpp, dpq, and dpb.

The absorption spectrum of the $[(\text{bpy})_2\text{Os}(\text{dpop})]^{2+}$ ion (Figure 1a) displays several maxima with the lowest energy absorption maximum at 786 nm ($\epsilon = 2.3 \times 10^3 \text{ M}^{-1} \text{ cm}^{-1}$) and a more intense peak at 553 nm ($\epsilon = 1.36 \times 10^4 \text{ M}^{-1} \text{ cm}^{-1}$). By analogy to spectra for similar $[(\text{bpy})_2\text{Os}(\text{BL})]^{2+}$ complex ions, and with the support of electrochemical results, these are assigned to $\text{Os}(\text{d}\pi) \rightarrow \text{dpop}(\pi^*)$ MLCT transitions. The absorption at 442 nm is assigned as an $\text{Os}(\text{d}\pi) \rightarrow \text{bpy}(\pi^*)$ MLCT transition by analogy to spectra for other $[(\text{bpy})_2\text{Os}(\text{BL})]^{2+}$ complex ions, while the higher energy maximum at 360 nm is most likely an $\text{Os}(\text{d}\pi) \rightarrow \text{dpop}(\pi^*)$ MLCT transition. An intense absorption shoulder near 295 nm and maximum at 289 nm are assigned to overlapping dpop and $\text{bpy}(\pi) \rightarrow (\pi^*)$ intraligand transitions.

The absorption spectrum of the bimetallic $[(\text{bpy})_2\text{Os}]_2(\text{dpop})^{4+}$ complex ion (Figure 1b) displays a peak in the near-IR spectrum at 1030 nm ($\epsilon = 1.16 \times 10^4 \text{ M}^{-1} \text{ cm}^{-1}$), with higher energy maxima at 696, 578, 439, 367, and 287 nm. A plot of $E_{1/2}$ for $\text{BL}^{0/-}$ ($\text{BL} = 2,3\text{-dpp}$, dpq, dpb, and dpop) in the respective bimetallic complexes versus lowest MLCT energies yields linear results ($r = 0.992$) using the 696 nm absorption as the data input for the $[(\text{bpy})_2\text{Os}]_2(\text{dpop})^{4+}$ ion. This suggests that the 696 nm absorption is the lowest energy $\text{Os}(\text{d}\pi) \rightarrow \text{dpop}(\pi^*)$ MLCT transition and is comparatively lower in energy than $^1\text{MLCT}$ transitions reported for similar complexes. The absorption at 1030 nm does not coincide with reported absorptions for $[(\text{bpy})_2\text{Os}]_2(\text{BL})^{4+}$ complexes where $\text{BL} = 2,3\text{-dpp}$, dpq, or dpb; however, absorption spectra for those complexes were not reported in the near-IR.⁷ The bimetallic $[(\text{bpy})_2\text{Os}]_2(2,5\text{-dpp})^{4+}$ has a similar intense absorption at 891 nm, which has been assigned as a $^3\text{MLCT}$ transition.⁴ Although intervalence transitions for mixed valent osmium species are found in the near-infrared spectrum, electrochemical study of the $[(\text{bpy})_2\text{Os}]_2(\text{dpop})^{4+}$ complex ion shows that it is stable in solution, and therefore the 1030 nm absorption is not the result of a mixed-valent species. We tentatively assign the 1030 nm absorption to a $\text{Os}(\text{d}\pi) \rightarrow \text{dpop}(\pi^*)$ $^3\text{MLCT}$ transition, in agreement with the assignment for the $[(\text{bpy})_2\text{Os}]_2(2,5\text{-dpp})^{4+}$ ion. The absorption maximum at 578 nm is also

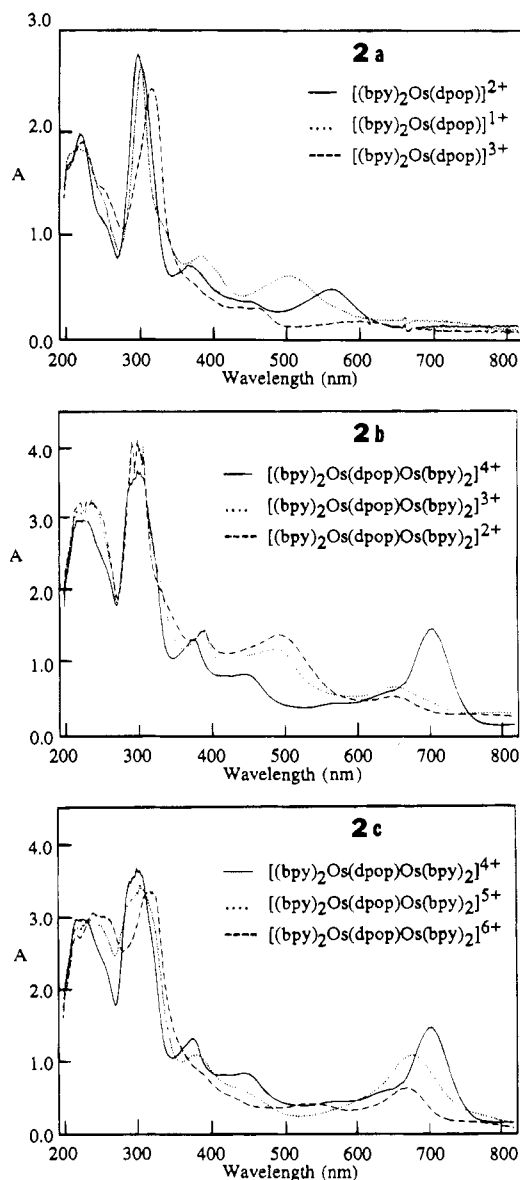


Figure 2. Spectroelectrochemical results for $[(\text{bpy})_2\text{Os}(\text{dpop})](\text{PF}_6)_2$ and $[(\text{bpy})_2\text{Os}]_2(\text{dpop})(\text{PF}_6)_4$ in CH_3CN (0.10 M Bu_4NPF_6): (a) spectra of $[(\text{bpy})_2\text{Os}(\text{dpop})](\text{PF}_6)_2$ and oxidized and reduced species; (c) spectra of $[(\text{bpy})_2\text{Os}]_2(\text{dpop})(\text{PF}_6)_4$ and one- and two-electron reduced species; (e) spectra of $[(\text{bpy})_2\text{Os}]_2(\text{dpop})(\text{PF}_6)_4$ and one- and two-electron oxidized species.

assigned to $\text{Os}(\text{d}\pi) \rightarrow \text{dpop}(\pi^*)$ MLCT transition on the basis of electrochemical results and by analogy with spectra for similar complexes, while the absorption at 439 nm is most likely due to a $\text{Os}(\text{d}\pi) \rightarrow \text{bpy}(\pi^*)$ MLCT transition. The absorption at 367 nm is slightly lower in energy than for monometallic complex and is consistent with assignment to a $\text{Os}(\text{d}\pi) \rightarrow \text{dpop}(\pi^*)$ MLCT transition. A higher energy shoulder and absorption maximum at 287 nm are again assigned to dpop and $\text{bpy}(\pi) \rightarrow (\pi^*)$ intraligand transitions.

Comparison of the spectra for the monometallic and bimetallic complexes show that $\text{Os}(\text{d}\pi) \rightarrow \text{dpop}(\pi^*)$ MLCT transitions and dpop intraligand transitions for the bimetallic complex occur at lower energy for the bimetallic species. This result is attributed to stabilization of the $\text{dpop}(\pi^*)$ orbitals upon coordination of the second $(\text{bpy})_2\text{Os}^{2+}$ fragment, and is consistent with electrochemical data that show a $\text{dpop}(\pi^*)$ orbital stabilization upon formation of the bimetallic species.

No detectable emission at $\lambda_{\text{em}} < 800$ nm was observed from deoxygenated room temperature acetonitrile solutions of

Table 2. Electronic Absorption Data for Some Mono and Bimetallic Osmium(II) Complexes^a

complex ion	λ_{\max} , nm	ϵ , $M^{-1} \text{ cm}^{-1} \times 10^{-3}$	assignment	ref
[(bpy) ₂ Os(dpop)] ²⁺	786	2.3	Os(d π) \rightarrow dpop(π^*)	MLCT this work
	553	13.6	Os(d π) \rightarrow dpop(π^*)	MLCT
	442	9.4	Os(d π) \rightarrow bpy(π^*)	MLCT
	360	19.4	Os(d π) \rightarrow dpop(π^*)	MLCT
	300(s)	90	dpop(π) \rightarrow (π^*)	IL
	289	95	bpy(π) \rightarrow (π^*)	IL
	486	12.7	Os(d π) \rightarrow 2,3-dpp(π^*)	MLCT 6
[(bpy) ₂ Os(2,3-dpp)] ²⁺	432(s)	11.0	Os(d π) \rightarrow bpy(π^*)	MLCT
	536	13.4	Os(d π) \rightarrow dpq(π^*)	MLCT 6
[(bpy) ₂ Os(dpq)] ²⁺	428	11.0	Os(d π) \rightarrow bpy(π^*)	MLCT
	570	13.8	Os(d π) \rightarrow dpb(π^*)	MLCT 6
[(bpy) ₂ Os(dpb)] ²⁺	446(s)	12.8	Os(d π) \rightarrow bpy(π^*)	MLCT
	408(s)	17.3	Os(d π) \rightarrow bpy(π^*)	MLCT
[((bpy) ₂ Os) ₂ (dpop)] ⁴⁺	1030	11.6	Os(d π) \rightarrow dpop(π^*)	MLCT this work
	920(s)	6.7	Os(d π) \rightarrow dpop(π^*)	MLCT
	696	31.7	Os(d π) \rightarrow dpop(π^*)	MLCT
	640(s)	12.6	Os(d π) \rightarrow dpop(π^*)	MLCT
	578	9.3	Os(d π) \rightarrow dpop(π^*)	MLCT
	439	17.4	Os(d π) \rightarrow bpy(π^*)	MLCT
	367	27.7	Os(d π) \rightarrow dpop(π^*)	MLCT
	310(s)	70	dpop(π) \rightarrow (π^*)	IL
	287	125	bpy(π) \rightarrow (π^*)	IL
	742	6.39	Os(d π) \rightarrow 2,3-dpp(π^*)	MLCT 4
	522	25.2	Os(d π) \rightarrow 2,3-dpp(π^*)	MLCT 7
[((bpy) ₂ Os) ₂ (2,3-dpp)] ⁴⁺	432	19.8	Os(d π) \rightarrow bpy(π^*)	MLCT
	891	12.4	Os(d π) \rightarrow 2,5-dpp(π^*)	MLCT 4
[((bpy) ₂ Os) ₂ (2,5-dpp)] ⁴⁺	799	9.75	Os(d π) \rightarrow 2,5-dpp(π^*)	MLCT 4
	616	27.0		
[((bpy) ₂ Os) ₂ (dpq)] ⁴⁺	630	20.9	Os(d π) \rightarrow dpq(π^*)	MLCT 7
	428	14.3	Os(d π) \rightarrow bpy(π^*)	MLCT
	398	19.6	Os(d π) \rightarrow dpq(π^*)	MLCT
[((bpy) ₂ Os) ₂ (dpb)] ⁴⁺	670	16.8	Os(d π) \rightarrow dpb(π^*)	MLCT 7
	610	12.9	Os(d π) \rightarrow dpb(π^*)	MLCT
	510	8.16	Os(d π) \rightarrow dpb(π^*)	MLCT
	422	16.6	Os(d π) \rightarrow bpy(π^*)	MLCT

^a All spectra were recorded in acetonitrile.

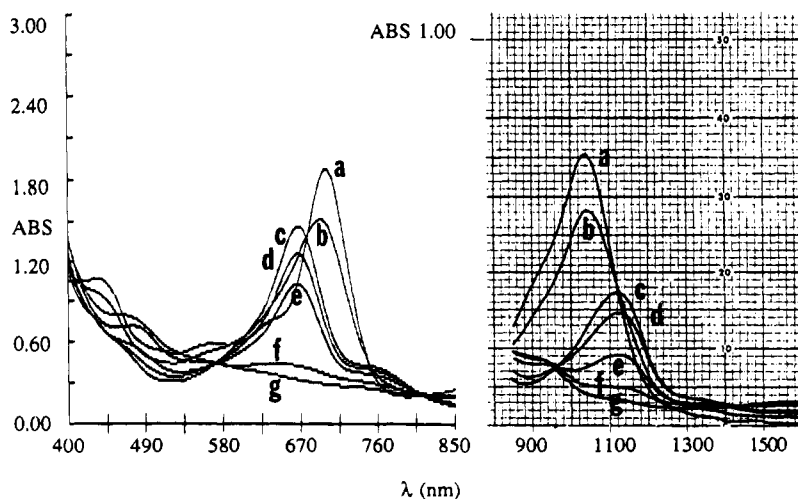


Figure 3. Visible and near-IR absorption spectra of $[(bpy)_2Os]_2(dpop)^{4+/5+/6+}$ throughout Ce^{4+} additions: plots a–c between 0 and 1 equiv; plots c–e between 1 and 2 equiv; plots f and g in excess of 2 equiv.

$[(bpy)_2Os(dpop)]^{2+}$ following excitation into the lowest energy MLCT absorption.

Spectroelectrochemistry. Since both the mono and bimetallic $[(bpy)_2Os]_{1,2}(dpop)^{2+,4+}$ ions could be reversibly electrochemically oxidized and reduced, electronic absorption spectra of several charged species were obtained and are shown in Figure 2.

The absorption spectrum of the oxidized $[(bpy)_2Os^{III}(dpop)]^{3+}$ ion shows a loss of intensity and red shift of the lowest energy peak relative to the $[(bpy)_2Os^{II}(dpop)]^{2+}$ absorption at 553 nm. The direction of the energy shift and loss of intensity are consistent with the assignment of absorptions in this region of

the spectrum for the original $[(bpy)_2Os^{II}(dpop)]^{2+}$ complex as $Os(d\pi) \rightarrow dpop(\pi^*)$ transitions. The complete loss of the 360 nm peak upon osmium oxidation (Figure 2a) suggests that the 360 nm absorption is due to a MLCT rather than intraligand transition. The absorption spectrum for the reduced $[(bpy)_2Os(dpop)]^+$ species shows a distinct absorption maximum at 500 nm which is assigned to a $dpop^-(\pi^*) \rightarrow (\pi^*)$ transition. The absorption spectrum for the $[(bpy)_2Os(dpop)]^0$ species recorded after the second reduction shows broadening between 425–475 nm in addition to retention of the 500 nm peak.

Absorption spectra for the reduced bimetallic $[(bpy)_2Os]_2(dpop)^{3+,2+}$ species show the growth of an intense absorption

near 490 nm for the one-electron reduction and broadening at 450 nm occurring upon the second reduction. These absorptions are assigned to $\text{dpop}^{-\cdot-2}(\pi^*) \rightarrow (\pi^*)$ intraligand transitions.

Successive oxidation of the $[(\text{bpy})_2\text{Os}]_2(\text{dpop})^{4+}$ ion produces several changes in the absorption spectrum. The absorption spectrum of the mixed valent $[(\text{bpy})_2\text{Os}]_2(\text{dpop})^{5+}$ species shows a blue shift and loss of intensity of the lowest energy absorption maximum and loss of absorptions at 640(s), 548, 439, and 367 nm, consistent with assignments as $\text{Os}(\text{d}\pi) \rightarrow \text{dpop}(\pi^*)$ and $\text{Os}(\text{d}\pi) \rightarrow \text{bpy}(\pi^*)$ MLCT transitions. The absorption spectrum of $[(\text{bpy})_2\text{Os}]_2(\text{dpop})^{6+}$ shows additional loss of absorption intensity of the lowest energy peak and the appearance of a 525 nm peak, again consistent with assignment as a $\text{Os}(\text{d}\pi) \rightarrow \text{dpop}(\pi^*)$ transition.

Intervalence Transition. The bimetallic $[(\text{bpy})_2\text{Os}]_2(\text{dpop})^{4+}$ ion in D_2O was oxidized chemically with $\text{Ce}(\text{NH}_4)_2(\text{NO}_3)_6$, and the electronic absorption spectrum recorded between 400 and 1600 nm (Figure 3). Throughout oxidation to yield the mixed-valence $[(\text{bpy})_2\text{Os}]_2(\text{dpop})^{5+}$ bimetallic ion, the lowest energy MLCT absorption maximum shifted from 1030 to 1120 nm with decreasing intensity, while the 696 nm absorption shifted to 665 nm with decreasing intensity. Isosbestic points were observed near 680, 810, and 1120 nm throughout the oxidation indicative of a single process occurring. The visible absorption spectrum of the chemically generated $[(\text{bpy})_2(\text{Os})_2(\text{dpop})]^{5+}$ in D_2O is the same within experimental variation, to the mixed valent spectrum produced electrochemically in CH_3CN (Figure 2). At the one electron equivalence point, absorptions at 750 and at 1120 nm ($\epsilon = 5500 \text{ M}^{-1} \text{ cm}^{-1}$; $\nu_{1/2} = 1700 \text{ cm}^{-1}$) were observed. Additional amounts of Ce^{4+} caused a decrease in the absorption maxima at both 665 and 1120 nm and loss of the initial isosbestic points. On the basis of the trends in absorption changes upon one- and two-electron

oxidation, the absorptions at 750 and 1120 nm for $[(\text{bpy})_2\text{Os}]_2(\text{dpop})^{5+}$ are tentatively assigned to intervalence transfer (IT) transitions.

The observed bandwidth of 1700 cm^{-1} is less than a value of 4520 cm^{-1} calculated for symmetric, homonuclear one-electron transfer processes according to equations derived by Hush.¹⁹

$$\Delta\nu_{1/2}(\text{calcd}) = [2.31 \times 10^3(\nu_{\text{max}})]^{1/2} (\nu \text{ in } \text{cm}^{-1})$$

Multiple IT absorptions have been reported for several hetero- and homobimetallic osmium complexes.^{7,9,15} A standard semi-quantitative method applied for calculating E_{SO} , the energy difference between spin-orbit states, based on energies of IT transitions has been developed²⁰ and applied to several mixed valent bimetallic osmium systems.^{7,9,15,20} Using IT values obtained from the spectrum of $[(\text{bpy})_2\text{Os}]_2(\text{dpop})^{5+}$, $E_{\text{SO},1} = E_{\text{IT},2} - E_{\text{IT},1}$ is calculated as $4,480 \text{ cm}^{-1}$ which is larger than $E_{\text{SO},1} = 3430 \text{ cm}^{-1}$ reported for $[(\text{bpy})_2\text{Os}]_2(2,3\text{-dpp})^{5+}$.⁷ The third IT transition is not experimentally observed, but would be expected at higher energy and may be obscured by more intense MLCT transitions.

Acknowledgment is made to the donors of the Petroleum Research Fund, administered by the American Chemical Society, for support of this work. We also wish to thank Professor Karen J. Brewer, Virginia Polytechnic and State University, for providing the $(\text{bpy})_2\text{OsCl}_2$, for conducting the spectroelectrochemistry experiments, and for valuable discussions.

IC941259J

(19) Hush, N. S. *Prog. Inorg. Chem.* **1967**, 8, 391.

(20) Kober, E. M.; Goldsby, K. A.; Narayana, D. N. S.; Meyer, T. J. *J. Am. Chem. Soc.* **1983**, 105, 4305.